Ultralow thermal conductivity of silicon nanowire arrays by molecular dynamics simulation

2017 Mater. Res. Express 4 025029

(http://iopscience.iop.org/2053-1591/4/2/025029)

Materials Research Express

RECEIVED
16 November 2016

REVISED
18 December 2016

ACCEPTED FOR PUBLICATION
10 January 2017

PUBLISHED
22 February 2017

PAPER

Ultralow thermal conductivity of silicon nanowire arrays by molecular dynamics simulation

Ting Zhang[1,2,3], Xue Xiong[4], Meng Liu[4], Guoan Cheng[3], Ruiting Zheng[3], Ju Xu[1] and Lei Wei[2]

[1] Institute of Electrical Engineering, Chinese Academy of Sciences, Beijing 100190, People's Republic of China
[2] School of Electrical and Electronic Engineering, Nanyang Technological University, Singapore 639798, Singapore
[3] College of Nuclear Science and Technology, Beijing Normal University, Beijing 100875, People's Republic of China
[4] Institute of Engineering Thermophysics, Chinese Academy of Sciences, Beijing 100190, People's Republic of China

E-mail: xuju@mail.iee.ac.cn **and** wei.lei@ntu.edu.sg

Keywords: thermal conductivity, silicon nanowire array, surface roughness, doping concentration, molecular dynamics

Abstract

We investigate the thermal conductivities of silicon nanowires (SiNWs) and their arrays based on molecular dynamics simulations. It is found that diminishing diameter, roughing surface and doping impurity of SiNWs can reduce their thermal conductivities by two or three orders of magnitude compared with that of bulk silicon crystals due to the strong phonon boundary and phonon impurity scattering. The simulated thermal conductivities of SiNW arrays demonstrate that arraying nanowires can further lower the thermal conductivity owing to the laterally-coupled effect, and the thermal conductivity of arrays decreases notably with the increased nanowire volume fraction, resulting in an ultralow thermal conductivity for the doped SiNW arrays with rough surfaces, which provides theoretical guidance of thermal management for semiconductor nanowire based microelectronic and thermoelectric devices.

1. Introduction

Silicon, the second-most abundant element in the earth's crust, has historically been considered as an excellent semiconductor material for microelectronic, optoelectronic, photovoltaic and sensing applications due to its nontoxicity, good stability at high temperature and mature processes for manufacturing electronic devices, but is an inefficient material for thermoelectric devices because of its high thermal conductivity of 150 W m^{-1} K^{-1} at room temperature [1]. However, in recent decades, both theoretical and experimental reports have demonstrated that SiNWs surprisingly possess low thermal conductivities [2–5], which is crucial for thermal management of silicon-based microelectronic devices and entitles silicon to the potential applications of thermoelectric power generation and cooling devices.

Theoretically, heat in silicon is mostly carried by phonon transport, even in the presence of high concentrations of charge carriers, so the enhancement of phonon scattering will be an effective way to reduce thermal conductivity [6]. Since doped SiNWs not only have the strong phonon-impurity scattering, but also own the intense phonon-boundary scattering due to the nanoscale dimensions that are much smaller than the phonon mean free path of bulk silicon (~300 nm) [7], thus the thermal conductivities of doped SiNWs are reduced by two or three orders of magnitude compared to that of bulk silicon [1]. It is reported that the 10-nm-wide nanowires with a doping level of 2.0×10^{20} cm^{-3} exhibit thermal conductivity as low as 0.76 W m^{-1} K^{-1} at 300 K [2], and the rough SiNWs with doping level of 2.8×10^{17} cm^{-3} show the thermal conductivity of 1.6 W m^{-1} K^{-1} at 300 K, even though the diameter of the tested nanowires is 52 nm [1], which indicates that roughening the surface of the nanowire can further reduce their thermal conductivities. For doped SiNW arrays, the thermal conductivity sharply decreased with the increase of its roughness and dives to 1.68 W m^{-1} K^{-1} at 300 K when doped boron atoms with the concentration of 2.0×10^{19} cm^{-3} [8]. Although the above experimental works have been carried on measuring the thermal conductivities of SiNWs and their arrays, the sample fabrication and the setup establishment are quite complicated and expensive due to the nanoscale measurement. More importantly, the thermal conductivities of SiNWs from experimental results are generally the integrated effect of many factors such as diameter, length, temperature, surface roughness and doping concentration. It is difficult to separate the

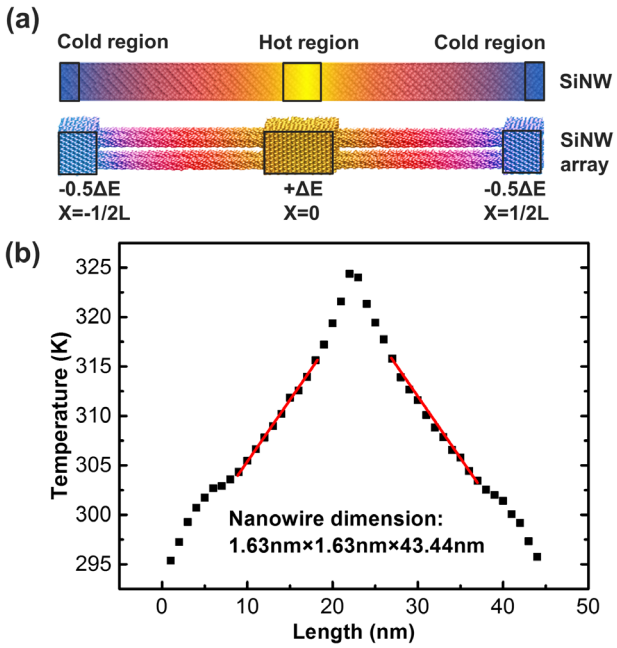

Figure 1. (a) Schematic diagrams for the 3D lattice configuration of individual SiNW and SiNW array. (b) Temperature profile in a SiNW and the solid linear fit (red) of the middle of the data.

contribution of each factor and conclude the change rule of thermal conductivity as the variation of each factor. Therefore, molecular dynamics (MD) simulation has become an important approach to study the microscopic process of heat transport in nanostructure materials and to predict the effect of each single factor on the thermal conductivity of nanostructure materials.

So far, a few MD simulations have been performed to investigate thermal conductivity of individual SiNWs as a function of cross-section area [9, 10], simulation temperature [11], isotope doping [12] and surface roughness [13–15]. However, there have been rare studies on thermal conductivities of impurity doped SiNWs with different surface roughness and their arrays by MD simulation. For many applications, doped p-type and n-type SiNW arrays with a large area would be more practical and efficient compared with an individual SiNW. Therefore, in this work, we systemically study the thermal conductivities of SiNWs with different lengths, diameters, surface roughness and doped concentration, and the thermal conductivities of SiNW arrays with different surface roughness, doped concentration, simulation temperature and volume fraction using the non-equilibrium molecular dynamics (NEMD) method. The results fully reveal that diminishing diameter, roughing surface, doping impurity and arraying nanowires are efficient ways to reduce the thermal conductivity of SiNW, which plays an important role in thermoelectric and microelectronic devices based on SiNWs and other semiconductor nanowires.

2. Methods

The NEMD simulation includes two approaches to predict the thermal conductivity, namely imposing heat flux and imposed temperature gradient [16]. Here we use the NEMD simulation where temperature gradient is obtained from the imposed heat flux. Specifically, the simulation systems of both single nanowire and four nanowire arrays are first divided into slices along the length direction, then a heat flux is created by imposing energy ΔE in the two center slices of the system as a heat source, and subtracting $0.5\Delta E$ from each slice at the two ends of the system as a heat sink shown in figure 1(a). This configuration allows us to ensure the energy conservation and to respect the periodic boundary conditions in the length direction of SiNW and its array (i.e. the direction of the heat flux). The temperature T_{MD} of each slice and its gradient between the heat source and heat sink are calculated in steady state using the energy equipartition theorem [17].

$$T_{\mathrm{MD}} = \frac{1}{3N_s k_{\mathrm{B}}} \sum_{i=1}^{N_s} m_i \langle v_i \rangle^2 \tag{1}$$

where $\langle\rangle$ stands for the averaging over the total simulation time, N_s is the number of atoms in the slice, and k_{B} is the Boltzmann constant. However, T_{MD} of equation (1) representing the real temperature is only valid at the temperatures higher than the Debye temperature. For silicon, the Debye temperatures is 645 K. Therefore, when

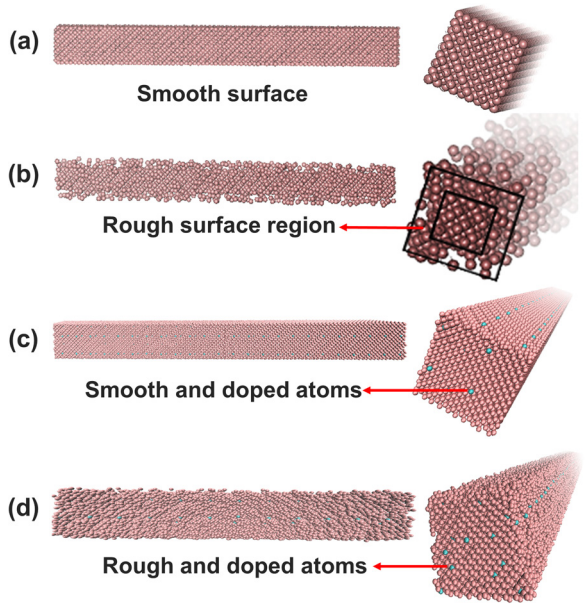

Figure 2. Four kinds of the SiNW configurations: (a) smooth surface, (b) rough surface, (c) smooth surface with doped atoms, and (d) rough surface with doped atoms.

the simulation temperature is smaller than 645 K, T_{MD} needs to be corrected considering quantum effects and calculated by the equation (2) [18].

$$\frac{3}{2}N_s k_B T_{MD} = \frac{1}{2}\int_0^{\omega_D} D(\omega)N(\omega, T)\hbar\omega \mathrm{d}\omega \tag{2}$$

where $D(\omega)$ is the Debye density of states, ω is the phonon frequency, and $N(\omega,T)$ is the phonon occupation number given by the Bose–Einstein distribution corresponding to the local equilibrium temperature T, also the quantized temperature.

According to Fourier's law, the effective thermal conductivity can be obtained by the formula

$$k_{MD} = -\frac{J}{\mathrm{d}T_{MD}/\mathrm{d}x} \tag{3}$$

where J is the heat flux density along the length direction of the SiNW, and it is expressed as $J = \Delta E A^{-1}$. For individual SiNW, A represents the sectional area of individual SiNW. While for SiNW arrays consisting of four SiNWs with same configuration as shown in figure 1(a), A is just the total sectional area of the four SiNWs rather than the sectional area of the built heating region. Figure 1(b) is a typical temperature distribution across the SiNW. Usually the temperature distribution near the hot and cold layer is non-linear, so the thermal conductivity is obtained from the red linear parts of the temperature distribution in the middle. Because the classic temperature is used in equation (3), a quantum correction needs be applied as equation (4).

$$k = k_{MD}\frac{\partial T_{MD}}{\partial T}. \tag{4}$$

In these NEMD simulations, we employ the Stillinger–Weber (SW) potential [19] which is one of the most widely used two-and three-body interatomic potentials for silicon to calculate the thermal conductivities of pure SiNWs and their arrays, and utilize the modified SW interatomic potential for Si–B and Si–P interactions [20] to simulate the thermal conductivities of doped SiNWs and their arrays. The crystal orientations for all the simulated systems are the [1 0 0], [0 1 0] and [0 0 1] directions in the diamond lattice corresponding to the x, y and z axes, and the length direction z axe is set as periodic boundary (p) conditions while x and y axes are shrink-wrapped boundary (s) conditions. The simulation used a time step of 0.5 fs with the equation of motion integrated in time with the velocity Verlet algorithm [21]. In order to obtain accurate results, the system is first equilibrated in constant NVT ensemble (fixed number of atoms N, volume V, and temperature T) to obtain the controlled temperature. One simulation usually takes at least 3000 000 steps, with many running more than 5000 000 time steps (2.5 ns) in the large-scale atomic/molecular massively parallel simulator (LAMMPS) [22]. The first 1200 000 steps are used to relax and allow the system to achieve a steady state, while the rest are used for statistical analyses.

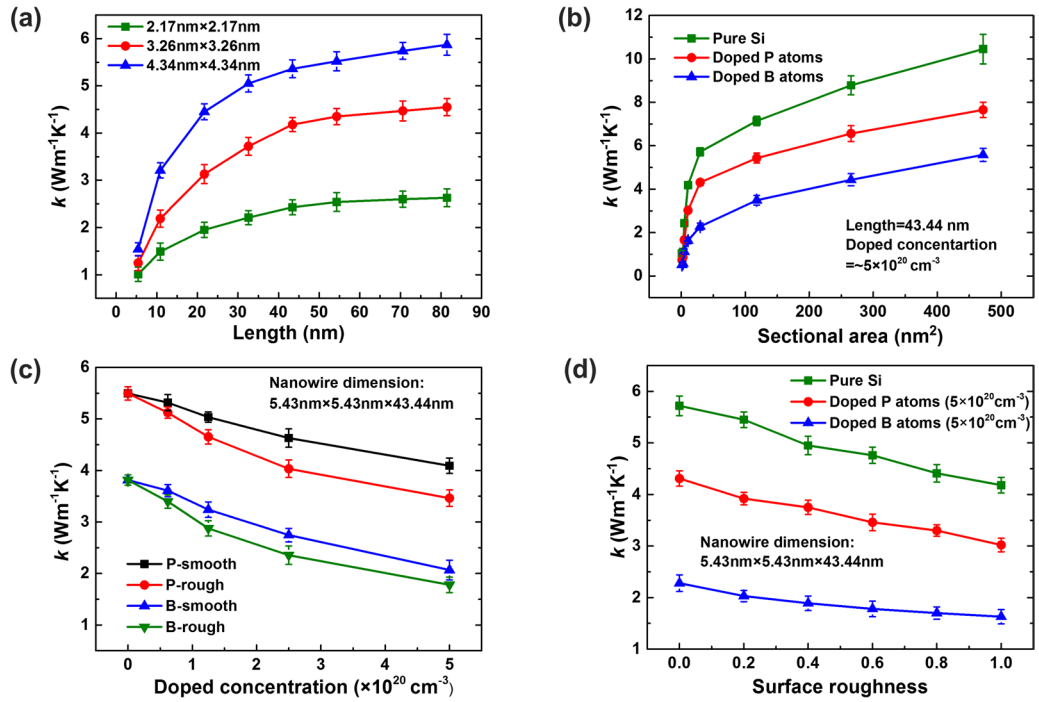

Figure 3. MD thermal conductivities at 300 K for different single SiNWs as a function of length (a), sectional area (b), doped P and B atom concentration (c) and surface roughness (d).

3. Results and discussion

Figure 2 shows four configurations of the SiNW used to simulate the thermal conductivities of individual SiNW and their arrays, including smooth surface, rough surface, smooth surface with doped atoms and rough surface with doped atoms. The doped atoms are introduced by randomly replacing Si atoms with a given quantity of phosphorus (P) and boron (B) atoms, while the rough surface is created by dividing one SiNW into two parts, namely the thick inner core and thin pseudo shell, and then deleting a certain percentage of atoms in the thin pseudo shell. In order to verify and eliminate the presence of the reported finite size effect in calculating thermal conductivity [9], we first calculate thermal conductivities of individual SiNW with three kinds of cross-section areas as a function of nanowire length at 300 K as shown in figure 3(a). The calculated value of thermal conductivity significantly increases with the increased simulated length and then starts to converge when the simulated length is larger than 30 nm. Volz and Chen calculated the thermal conductivity of SiNWs by EMD based on the Green–Kubo relation with both rigid and shrink-wrapped boundary conditions [9], and found that the thermal conductivity did not depend on the length of the SiNW when it was longer than 8.6 nm with a cross-sectional area of smaller than 28.62 nm^2. The difference of the critical value is mainly resulted from our different NEMD method and boundary conditions. As Yang *et al* reported [23], the convergence of the thermal conductivity exists in the simulation system with the sss and ssp boundary, and disappear in the ppp boundary. They also reported that a transition occurred in the thermal conductivity versus length curve after the initial convergence trend appeared near the mean free path of bulk silicon. However, due to the relative short simulation length, the transition is not observed in our results. In order to overcome the finite size effect on the calculated thermal conductivity, we use the simulated length with the minimum of 26.06 nm in the following simulations. Figure 3(a) also exhibits the thermal conductivity of SiNW increases with the increase of its sectional area under the same length. Thus, for comparison, we also simulate thermal conductivities of the three SiNWs consisting of pure Si, doped P and B atoms with the concentration of ~5 $\times$ 10^{20} cm^{-13} under the conditions of the different sectional area and the same simulated length of 43.44 nm at 300 K as shown in figure 3(b). The results indicate that the thermal conductivity of SiNW drops sharply with shrinking nanowire cross-section due to the intense phonon boundary scattering and that the doped SiNWs possess lower thermal conductivity than pure SiNW due to the strong phonon impurity scattering. The pure SiNW with a cross-section of 21.72 nm $\times$ 21.72 nm exhibits a k value of 10.45 W m^{-1} K^{-1}, while the k values of the same size SiNWs doped with 5 $\times$ 10^{20} cm^{-3} P and B atoms are 7.65 W m^{-1} K^{-1} and 5.58 W m^{-1} K^{-1}, respectively, which are close to the reported experimentally measured value of 3.5 W m^{-1} K^{-1} for the smooth SiNW with the diameter of 20 nm and the B atoms doping concentration of 2 $\times$ 10^{20} cm^{-13} [2]. Because phonon scattering by substitutional dopants can be attributed to the atomic mass and atomic radius differences between the host and dopant atoms namely mass disorder and lattice strain effects [20],

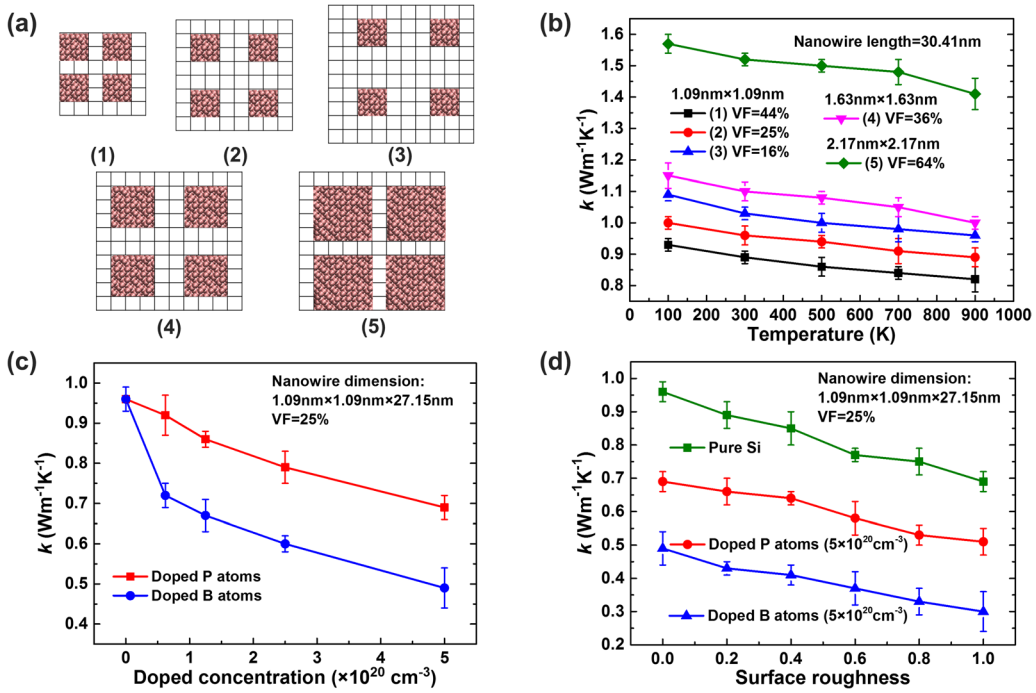

Figure 4. MD thermal conductivity for SiNW array. (a) Schematic diagram of SiNW arrays with the volume fraction of 44% (1), 25% (2), 16% (3), 36% (4) and 64% (5). MD thermal conductivities for SiNW arrays with different volume fraction at different temperatures (b), and with different doped concentration (c) and surface roughness (d) at 300 K.

and the effects in B-doped SiNWs are more significant than those in P-doped SiNWs, therefore, B-doped SiNWs show the lowest thermal conductivity compared with pure SiNWs and P-doped SiNWs under the same doping concentration.

In order to further enhance phonon boundary scattering and reduce thermal conductivity, we compute thermal conductivities of both smooth and rough SiNWs with different doping concentration of P and B atoms at 300 K as shown in figure 3(c). Herein, for the nanowire size of 5.43 nm × 5.43 nm × 43.44 nm (10 × 10 × 80 unit cell), the inner 6 × 6 × 80 unit cells are set as the core and the outer 4 × 4 × 80 unit cells are defined as the pseudo shell. The roughness of 0.6 with dimensionless unit is accomplished by deleting 60% of the atoms in the shell region, and all the surface roughness of the SiNW in figure 3(c) are 0.6. As the doped concentration of the SiNW increases, the thermal conductivity decreases correspondingly and rough SiNW has lower thermal conductivity than that of smooth SiNW, which demonstrates roughing surface is an effective way to reduce the thermal conductivity of SiNW. The calculated thermal conductivity is as low as 1.78 W m^{-1} K^{-1} at 300 K for B atoms doped SiNW with the roughness of 0.6 and the concentration of 5 × 10^{20} cm^{-3}, which approaches the measured thermal conductivity of 1.6 W m^{-1} K^{-1} at room temperature for the highly doped and rough SiNW with the diameter of 52 nm [1]. Figure 3(d) summarizes the effect of different surface roughness on the thermal conductivities of pure SiNW, P-doped SiNW and B-doped SiNWs with doping concentration of 5 × 10^{20} cm^{-3}. The roughness of 1.0 means that the SiNW just consists of the inner core without outer shell. The results reveal that thermal conductivity decreases nearly lineally with the increase of surface roughness.

Through adjusting the diameter and the interval of the SiNW, we also establish SiNW arrays with different volume fractions as shown in figure 4(a). The 1.09 nm × 1.09 nm SiNW (2 × 2 unit cell) with the interval of 1, 2 and 3 unit cell under the boundary condition of ppp can realize that the volume fraction of SiNW array is 44%, 25% and 16% (figure 4(a) (1)–(3)) respectively, while the 1.63 nm × 1.63 nm SiNW with the interval of 2 unit cell and the 2.17 nm × 2.17 nm SiNW with the interval of 1unit cell can accomplish the volume fraction of 36% and 64% (figure 4(a) (4) and (5)) respectively. The calculated results in figure 4(b) shows thermal conductivities of SiNW arrays slightly decline as the increased simulated temperature which agrees well with the MD results of single SiNW obtained by Galli *et al* [11]. It is more important that the thermal conductivity of SiNW array is smaller than that of the corresponding individual SiNW and decreases with the increased volume fraction. For example, the thermal conductivity of the single 2.17 nm × 2.17 nm SiNW is 2.08 W m^{-1} K^{-1} at 300 K, while the 2.17 nm × 2.17 nm SiNW array with the volume fraction of 64% exhibits the thermal conductivity of 1.52 W m^{-1} K^{-1} at 300 K. Moreover, the thermal conductivity of the 1.09 nm × 1.09 nm SiNW array is 1.03 W m^{-1} K^{-1} at 300 K for the volume fraction of 16% and 0.89 W m^{-1} K^{-1} for the volume fraction of 44%. This phenomenon is similar with the calculated results based on phonon transport theory that the thermal conductivity of nanowire array is considerably decreased with the enlarged nanowire volume fraction due to the

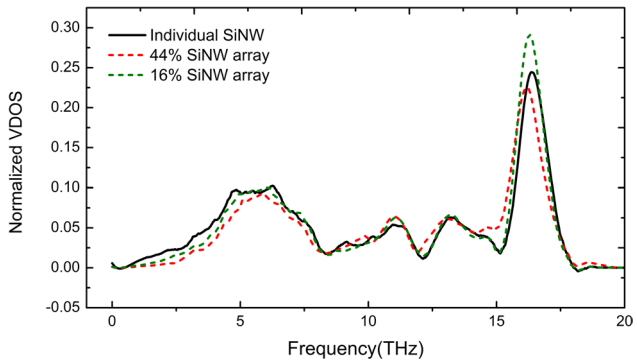

Figure 5. VDOS of the individual SiNW and SiNW arrays with the volume fraction of 16% and 44% at 300 K.

laterally-coupled effect [24]. Specifically, the increased nanowire volume fraction leads to high interface density in the lateral direction, scattering the phonons away and preventing them from directionally transferring the energies, thus resulting in the reduced phonon mean free path and thermal conductivity. By doping B and P atoms, we also obtain the thermal conductivities of the 1.09 nm $\times$ 1.09 nm $\times$ 27.15 nm SiNW array with different doping concentrations. Similar to single doped SiNW, the thermal conductivity of doped SiNW array decrease with the increased doping concentration, and B atoms doped array has a lower thermal conductivity than P atoms doped array with the same concentration. The thermal conductivity of the 1.09 nm $\times$ 1.09 nm $\times$ 27.15 nm SiNW array with doped B atom concentration of 5×10^{20} cm^{-3} is 0.49 W m^{-1} K^{-1} at 300 K, which has a magnitude equal to that of the isotope doping SiNW with the atom's percentages of 50% [12]. However, Zheng *et al* experimentally reported that the thermal conductivity is as low as 1 W m^{-1} K^{-1} for the rough SiNW array even though the doping concentrations is only 10^{18} cm^{-3} and the average diameter of SiNW is over 100 nm [25]. Therefore, we finally simulate the thermal conductivities of the pure SiNW arrays and doped SiNW arrays with the concentration of 5×10^{20} cm^{-3} as a function of its surface roughness. The results in figure 4(d) show that increasing surface roughness further reduces the thermal conductivity of the doped SiNW arrays. To further understand the origin of thermal conductivity reduction in SiNW array, we calculated the phonon or vibrational density of states (VDOS) by Fourier transform of the velocity autocorrelation function [26]. Figure 5 shows the VDOS of the individual SiNW and SiNW arrays with the volume fraction of 16% and 44% at 300 K. It is evident that the peaks of SiNW arrays shift to lower frequency compared with that of the individual SiNW, and the attenuation of low-frequency modes in SiNW arrays can be easily identified especially under 8 THz. These can be attributed to the fact that laterally-coupled effect exists in SiNW array, which brings the additional phonon scattering. Considering low frequency mode is the major contribution to heat transport in Si, therefore, the further reduction of thermal conductivity in SiNW arrays can be obtained.

4. Conclusion

In conclusion, this study shows that the thermal conductivity of SiNW decreases with the shrinking nanowire cross-section and the increased surface roughness due to the intense phonon boundary scattering, and the B-doped SiNW has a lower thermal conductivity than that of pure SiNW and P-doped SiNWs due to the strong phonon impurity scattering from mass disorder and lattice strain effects. Moreover, owing to the laterally-coupled effect in an SiNW array, the thermal conductivity of an SiNW array is smaller than that of an individual SiNW and decreases with enlarged nanowire volume fraction, yielding an ultralow thermal conductivity of the doped SiNW arrays with rough surface. The results provide a guideline for designing semiconductor nanowires and nanowire arrays with desired thermal conductivity by tuning their diameter, surface roughness, doping concentration and volume fraction, which offers a substantial impact on future developments of nanowire based thermoelectric and microelectronic devices.

Acknowledgments

Support for this work by the Chinese Academy of Science 'Hundred Talents' project of Y440411C41 and National Natural Science Foundation of China (Grant No. 51336009). This work is supported in part by the Singapore Ministry of Education Academic Research Fund Tier 2 (MOE2015-T2-1–066, MOE2015-T2-2–010), and Nanyang Technological University (Start-up grant M4081515: Lei Wei).

References

[1] Hochbaum A I, Chen R, Delgado R D, Liang W, Garnett E C, Najarian M, Majumdar A and Yang P 2008 Enhanced thermoelectric performance of rough silicon nanowires *Nature* **451** 163–7

[2] Boukai A I, Bunimovich Y, Tahir-Kheli J, Yu J-K, Goddard Iii W A and Heath J R 2008 Silicon nanowires as efficient thermoelectric materials *Nature* **451** 168–71

[3] Chen R, Hochbaum A I, Murphy P, Moore J, Yang P and Majumdar A 2008 Thermal conductance of thin silicon nanowires *Phys. Rev. Lett.* **101** 105501–4

[4] Li D, Wu Y, Kim P, Shi L, Yang P and Majumdar A 2003 Thermal conductivity of individual silicon nanowires *Appl. Phys. Lett.* **83** 2934–6

[5] Ponomareva I, Srivastava D and Menon M 2007 Thermal conductivity in thin silicon nanowires: phonon confinement effect *Nano Lett.* **7** 1155–9

[6] Asheghi M, Kurabayashi K, Kasnavi R and Goodson K 2002 Thermal conduction in doped single-crystal silicon films *J. Appl. Phys.* **91** 5079–88

[7] Ju Y and Goodson K 1999 Phonon scattering in silicon films with thickness of order 100 nm *Appl. Phys. Lett.* **74** 3005–7

[8] Zhang T, Wu S-l, Zheng R-t and Cheng G-a 2013 Significant reduction of thermal conductivity in silicon nanowire arrays *Nanotechnology* **24** 505718

[9] Volz S G and Chen G 1999 Molecular dynamics simulation of thermal conductivity of silicon nanowires *Appl. Phys. Lett.* **75** 2056–8

[10] Wang S C, Liang X G, Xu X H and Ohara T 2009 Thermal conductivity of silicon nanowire by nonequilibrium molecular dynamics simulations *J. Appl. Phys.* **105** 014316

[11] Donadio D and Galli G 2010 Temperature dependence of the thermal conductivity of thin silicon nanowires *Nano Lett.* **10** 847–51

[12] Yang N, Zhang G and Li B 2007 Ultralow thermal conductivity of isotope-doped silicon nanowires *Nano Lett.* **8** 276–80

[13] Sansoz F 2011 Surface faceting dependence of thermal transport in silicon nanowires *Nano Lett.* **11** 5378–82

[14] Liu L and Chen X 2010 Effect of surface roughness on thermal conductivity of silicon nanowires *J. Appl. Phys.* **107** 033501–5

[15] Donadio D and Galli G 2009 Atomistic simulations of heat transport in silicon nanowires *Phys. Rev. Lett.* **102** 195901–4

[16] Cruz C A, Termentzidis K, Chantrenne P and Kleber X 2011 Molecular dynamics simulations for the prediction of thermal conductivity of bulk silicon and silicon nanowires: Influence of interatomic potentials and boundary conditions *J. Appl. Phys.* **110** 034309

[17] Volz S G and Chen G 2000 Molecular-dynamics simulation of thermal conductivity of silicon crystals *Phys. Rev.* B **61** 2651–6

[18] Maiti A, Mahan G and Pantelides S 1997 Dynamical simulations of nonequilibrium processes—Heat flow and the Kapitza resistance across grain boundaries *Solid State Commun.* **102** 517–21

[19] Stillinger F H and Weber T A 1985 Computer simulation of local order in condensed phases of silicon *Phys. Rev.* B **31** 5262–71

[20] Lee Y and Hwang G S 2012 Mechanism of thermal conductivity suppression in doped silicon studied with nonequilibrium molecular dynamics *Phys. Rev.* B **86** 075202–6

[21] Martys N S and Mountain R D 1999 Velocity Verlet algorithm for dissipative-particle-dynamics-based models of suspensions *Phys. Rev.* E **59** 3733–6

[22] Plimpton S 1995 Fast parallel algorithms for short-range molecular dynamics *J. Comput. Phys.* **117** 1–19

[23] Yang X M, To A C and Tian R 2010 Anomalous heat conduction behavior in thin finite-size silicon nanowires *Nanotechnology* **21** 155704

[24] Zhang Y, Shi Y, Pu L, Wang J, Pan L and Zheng Y 2011 Enhancement of thermoelectric figure-of-merit in laterally-coupled nanowire arrays *Phys. Lett.* A **375** 2728–32

[25] Weisse J M, Marconnet A M, Kim D R, Rao P M, Panzer M A, Goodson K E and Zheng X L 2012 Thermal conductivity in porous silicon nanowire arrays *Nanoscale Res. Lett.* **7** 1–5

[26] Kohanoff J 1994 Phonon spectra from short non-thermally equilibrated molecular dynamics simulations *Comput. Mater. Sci.* **2** 221–32